Food and Chemical Toxicology 130 (2019) 22–31

Contents lists available at ScienceDirect

Food and Chemical Toxicology

journal homepage: www.elsevier.com/locate/foodchemtox

Metabolism and disposition of arsenic species from controlled dosing with dimethylarsinic acid (DMA^V) in adult female CD-1 mice. V. Toxicokinetic studies following oral and intravenous administration

Nathan C. Twaddle, Michelle Vanlandingham, Frederick A. Beland, Daniel R. Doerge*

Division of Biochemical Toxicology, National Center for Toxicological Research, U.S. Food and Drug Administration, Jefferson, AR, 72079, USA

ARTICLE INFO

Keywords:
Arsenic
Toxicokinetics
Dimethylarsinic acid
Metabolism

ABSTRACT

Arsenic species contaminate food and water, with typical dietary intake below 1 μg/kg bw/d. Exposure to arsenic in heavily contaminated drinking water is associated with human diseases, including cardiovascular and respiratory disorders, diabetes, and cancer. Dietary intake assessments show that rice and seafood are the primary contributors to intake of both inorganic arsenic and dimethylarsinic acid (DMA^V) and at similar magnitudes. DMA^V plays a central role in the toxicology of arsenic because enzymatic methylation of arsenite produces DMA^V as the predominant metabolite, which may promote urinary clearance but also generates reactive intermediates, predominantly DMA^{III}, that bind extensively to cellular thiols. Both inorganic arsenic and DMA^V are carcinogenic in chronically exposed rodents. This study measured pentavalent and trivalent arsenic species in blood and tissues after oral and intravenous administration of DMA^V (50 μg As/kg bw). DMA^V underwent extensive first-pass metabolism in the intestine and liver, exclusively by reduction to DMA^{III}, which bound extensively to blood and tissues. The results confirm a role for methylation-independent reductive metabolism in producing fluxes of DMA^{III} that presumably underlie arsenic toxicity and indicate the need to include all dietary intake of inorganic arsenic and DMA^V in risk assessments.

1. Introduction

Arsenic is a toxic element distributed ubiquitously throughout the earth's crust, predominantly as its inorganic forms (i.e., arsenate and arsenite) in soil and water (reviewed in Zhu et al., 2014). Metabolism of inorganic arsenic (As^i) to numerous organic forms occurs in many forms of terrestrial and marine life, including microbiota, plants, and animals (reviewed in Zhu et al., 2014; Taylor et al., 2017). Humans consume As^i from contaminated drinking water, which contains predominantly arsenate, and food, which contains both inorganic and organic arsenic. While typical dietary exposure to As^i is below 1 μg/kg bw/d in most developed world settings, heavily contaminated drinking water sources in the developing world (i.e., up to 1 mg/l; Mukherjee et al., 2006) can produce estimated daily intakes of up to 50 μg/kg bw/d. Exposure to arsenic is a major public health concern worldwide based on associations with many important human diseases (e.g., cardiovascular, pulmonary, and metabolic diseases and cancer) from epidemiological investigations and toxicity in experimental animal models (European Food Safety Authority, 2009; U.S. Environmental Protection Agency, 2010; World Health Organization, 2011; U.S. Food and Drug Administration, 2016).

The redox chemistry of As^i favors pentavalent arsenate in aerobic milieu, like soil and water, but the reducing environment in most cellular life facilitates formation of trivalent species, like arsenite (Zhu et al., 2014). The toxicity of arsenite itself manifests from its facile reactivity with thiols present in structural, functional, and regulatory proteins (Go and Jones, 2013; Shen et al., 2013) and low molecular weight compounds (e.g., reduced glutathione, GSH; Spuches et al., 2005). Moreover, metabolism of As^i appears central to the toxic effects by producing additional trivalent arsenic intermediates and pentavalent arsenic products (Scheme; Twaddle et al., 2018a; Twaddle et al., 2018b; Twaddle et al., 2019). Indeed, evidence supports roles for both methylation of arsenite by arsenite methyltransferase (As3MT; Dheeman et al., 2014; Currier et al., 2016) and direct reduction of pentavalent arsenic species (Delnomdedieu et al., 1994; Stýblo et al., 1997; Németi and Gregus, 2013; Twaddle et al., 2018a, 2018b, 2019) in the formation and binding of reactive trivalent arsenic species, even in tissues with low As3MT activity (Kobayashi et al., 2007). However, the evidence for metabolic activation of As^i by methylation is seemingly paradoxical, given that As3MT-catalyzed methylation appears to facilitate urinary

* Corresponding author.
E-mail address: daniel.doerge@fda.hhs.gov (D.R. Doerge).

https://doi.org/10.1016/j.fct.2019.04.045
Received 18 March 2019; Received in revised form 23 April 2019; Accepted 24 April 2019
Available online 12 May 2019

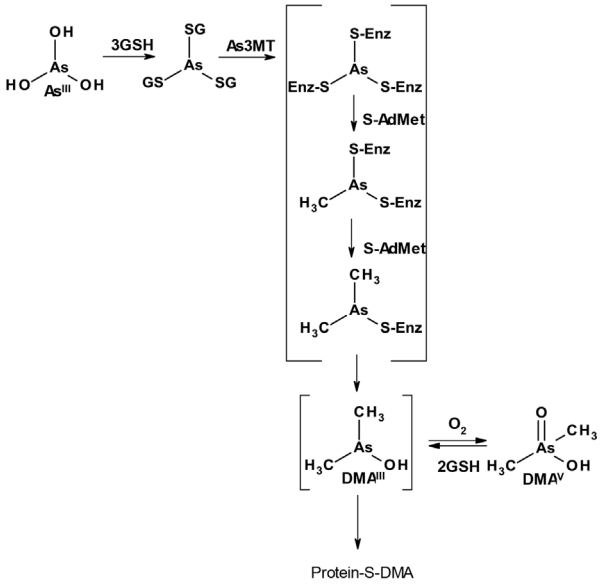

GSH = reduced glutathione
As3MT = arsenite methyltransferase
Enz-S = As3MT catalytic cysteine residues
S-AdMet = S-adenosylmethionine

Scheme. Metabolic activation to DMA^{III} by arsenite methyltransferase-(As3MT) catalyzed methylation of arsenite and direct reduction of DMA^{V}.

excretion of the major metabolite, dimethylarsinic acid (DMA^{V}), and decrease acute toxicity in wild-type vs. As3MT-knockout mice (Currier et al., 2016). The paradoxical relationship between metabolism and toxicity is underscored further by the observations that DMA^{V} and As^{i} are both carcinogenic when administered chronically to adult rodents (Wei et al., 2002; Arnold et al., 2006; Tokar et al., 2012).

Additionally, organic forms of arsenic contribute significantly to human intake of total arsenic. Rice is a major staple food, which through a confluence of soil chemistry, plant biology, and agricultural practices absorbs and translocates significant amounts of inorganic and methylated arsenic species into the grain (Zhao et al., 2013). The distribution between As^{i} and methylated forms, primarily DMA^{V}, varies widely as the percentages in rice can range from 90–0 and 10–100, respectively (Zhao et al., 2013). For example, in the general population of Japan, the ratio of DMA^{V}, relative to As^{i}, from dietary intake of grains (presumably primarily rice) is approximately 0.2 (3.3 vs. 13 μg As/day; Oguri et al., 2014), whereas in the U.S., the corresponding ratio from rice consumption is 1.4 (0.044 vs. 0.032 μg/kg bw As/d; U.S. Food and Drug Administration, 2016). Seafood is another major dietary source of organic arsenic (reviewed in Taylor et al., 2017). While arsenobetaine is the prominent As species present in fish, it is metabolically inert and has negligible toxicity (Taylor et al., 2017). Pioneering work by Francesconi and colleagues has elucidated two major classes of organic arsenic species present in seafood, arsenolipids and arsenosugars (Raml et al., 2009; Glabonjat et al., 2014; Al Amin et al., 2018). Quantitative analytical methodology is becoming more widely available, facilitating a more complete assessment of the total dietary intake of these forms of arsenic in seafood (Al Amin et al., 2018; Wolle and Conklin, 2108). The estimated daily intake in Japan from algae plus fish and shellfish for arsenolipids was 7.8 μg As per person and 4.8 μg As per person for arsenosugars (Al Amin et al., 2018). There is limited evidence in vitro for possible toxicity associated with some arsenolipids, but not arsenosugars (reviewed in Taylor et al., 2017); however, both arsenosugars and arsenolipids in seafood can be extensively converted by humans into DMA^{V} (Schmeisser et al., 2006; Raml et al., 2009). Finally, DMA^{V} (cacodylic acid) is also used as a non-selective herbicide (Kenyon et al., 2005).

Despite, or possibly because of, the complexities conferred by metabolism and dietary exposure to multiple forms of arsenic-containing compounds, risk assessments by international regulatory bodies have focused on exposures to As^{i}, based primarily on increased incidences of cancer in humans consuming elevated levels of As^{i} from heavily contaminated drinking water (European Food Safety Authority, 2009; U.S. Environmental Protection Agency, 2010; World Health Organization, 2011; U.S. Food and Drug Administration, 2016). The centrality of internal exposure to DMA^{V} in arsenic toxicity, from either metabolism of As^{i} or direct consumption, suggest that the basis for risk assessment should include dietary sources of DMA^{V}.

In order to compare the internal exposures associated with metabolic activation of As^{i} vs. DMA^{V}, the current study used controlled dosing with DMA^{V} in adult female CD-1 mice with identical methodology to that used in a previous toxicokinetic study with arsenite (Twaddle et al., 2018b). Female mice were selected to maintain continuity with previous studies that specifically investigated pharmacokinetics during perinatal lifestages (i.e., placental and lactational transfer and neonatal). While no compelling evidence for sex differences in arsenite pharmacokinetics between males and females is known, additional testing of this hypothesis may be required. The administered dose in both cases was 50 μg/kg bw as As equivalents, which was chosen to minimize non-linear effects on toxicokinetics caused by metabolic saturation at higher doses (Kenyon et al., 2005; Hughes et al., 2008; Twaddle et al., 2018a). Furthermore, this comparison provides a direct testing of the hypothesis that As3MT-independent reductive metabolism of pentavalent arsenic species contributes to the formation and binding of trivalent intermediates that presumably underlie the toxicity of arsenic (Go and Jones, 2013; Shen et al., 2013; Scheme).

2. Methods

2.1. Reagents and standards

Hydrogen peroxide (30%) was purchased from Fisher Optima (Thermo Fisher Scientific, Waltham, MA); ammonium phosphate dibasic from Sigma-Aldrich (St. Louis, MO); MilliQ-H_2O (18 MΩ) from Millipore (Billerica, MA); and 30 kDa molecular weight cutoff centrifuge filters (30 kD MWCO) from EMD Millipore (Darmstadt, Germany). Blood was collected in EDTA-coated plasma separator tubes (MiniCollect, Greiner Bio-One, Monroe, NC) ranging in size from 0.25 to 1 mL.

NIST-certified solutions (standard reference materials, SRMs) of arsenite and arsenate were purchased from SPEX (Metuchen, NJ DMA^{V} (dimethylarsinic acid) was purchased from Chem Service (West Chester, PA), sodium arsenite was purchased from Lab Chem (Zelienople, PA), and all solutions were prepared by accurately weighing a portion and diluting with MilliQ-H_2O. All dilutions were prepared in dark, polypropylene bottles and stored at 4 °C. All standards were prepared on the basis of elemental As concentration (75 g/mol) and analyzed by infusion into the ICP/MS to ensure an equal As concentration, using arsenate as the reference (NIST SRM 1640A, trace elements in natural water; Gaithersburg, MD). Sterile saline used for preparation of the intravenous dosing solution was obtained from Vedco, Inc. (St. Joseph, MO).

2.2. Animal handling procedures

All procedures involving the care and handling of mice were reviewed and approved by the National Center for Toxicological Research Laboratory Animal Care and Use Committee. Charles River Co. (Wilmington, MA) provided female CD-1 mice (9–10 weeks of age). Upon arrival, mice were placed on a low-arsenic basal diet (5K96, Test Diets, Purina Mills, Richmond, IN) for at least 10 days in order to reduce the background levels of arsenic present in blood and tissues. This

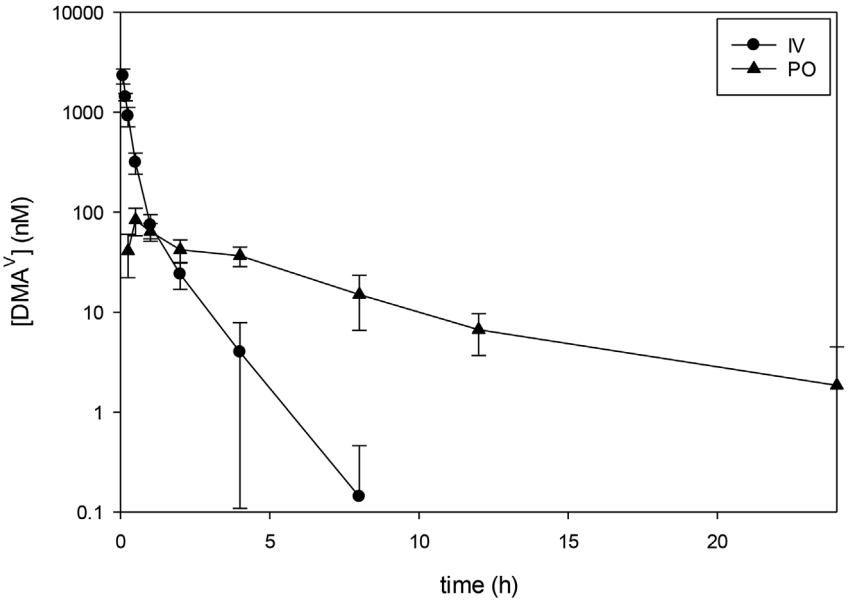

Fig. 1. Plasma time course data for DMA^V in female CD-1 mice dosed orally (PO) and intravenously (IV) with 50 μg/kg bw DMA^V (arsenic equivalents; values plotted represent means of n = 5–6 mice per time point ± SD). The LOD was approximately 1 nM in blood (50 μL).

length of depuration time was not rigorously investigated but found to be sufficient in our initial study (Twaddle et al., 2018a). Adult mice were dosed with DMA^V by gavage (n = 54) or intravenously (IV; n = 60) via the lateral tail vein (5 μL/g bw) at 9–10 weeks of age when the body weights were 27.5 ± 5.1 or 28.5 ± 4.2 g (mean ± SD), respectively. A dose of 50 μg/kg bw as As equivalents (667 nmol/kg bw) was used throughout. All mice had access to chow throughout the procedures. Blood was collected by cardiac puncture after CO_2 asphyxiation at various times after dosing (pre-dose, dosing at 0 min, 0.083 (5 min, IV only), 0.167 (10 min, IV only), 0.25 (15 min), 0.5 (30 min), 1, 2, 4, 8, and 24 h for the preparation of plasma and erythrocyte fractions by centrifugation (n = 6 mice per time point for gavage and n = 5–6 mice per time point for IV). Tissues were collected from all mice 1 h after dosing because this interval produced maximal tissue levels after gavage administration in the previous studies (Twaddle et al., 2018a). This sampling time was used to maintain methodological continuity with interpretations from the previous studies and also because plasma levels of DMA^V were essentially maximal at 0.5–1 h (Fig. 1) and maximal levels of DMA^{III} were observed in erythrocytes at 1 h (Fig. 2). Tissue and blood samples were stored frozen at −60 °C until analyzed. Repeated analysis of selected blood and tissue samples stored at −60 °C over the course of several months showed no evidence for significant changes in the determined concentrations of any arsenic species.

For gavage treatment, the dosing solution was prepared by accurately weighing DMA^V, diluting with MilliQ H_2O into a dark, polypropylene bottle, and storing in the refrigerator until use. The dosing solution for the IV exposure study was prepared and stored similarly to the gavage study; however, the diluent was sterile saline. Concentrations of both dosing solutions were measured and observed to be stable throughout the duration of each exposure route study.

2.3. Sample preparation procedures

Plasma, erythrocytes, and tissues were processed as previously described (Twaddle et al., 2018a). All samples were analyzed with and without H_2O_2 treatment using LC-ICP/MS to separate and quantify soluble DMA^V. The entire length of the intestine, from just below the stomach to the rectum, was collected. Representative tissue samples were obtained by taking portions throughout the respective organs. No special perfusion procedures were used to purge any included contents from the tissues (e.g., blood and feces) based on prior experimentation showing no evidence for carryover into enterocytes or luminal contents from oral arsenite dosing (Twaddle et al., 2018b). The time courses and excretion data following orally administered arsenite gavage showed minimal concentrations of speciated arsenic species in feces (mean 2 ± 2% of total dose, primarily as DMA^V, 87%; Twaddle et al., 2018a) and similar profiles of arsenic species in perfused (Gokulan et al., 2018) vs. unperfused (Twaddle et al., 2018b) intestinal tissue following oral administration of arsenite. Specifically, similar percentages of total intestinal arsenic species present as either DMA(III + V), MMA(III + V), or As3 + As^i-bound were observed in perfused intestine (53, 34, 14%, respectively, from repeated oral dosing through drinking water in Gokulan et al., 2018) vs. unperfused intestine (30, 53, 17%, respectively, from single gavage dosing in Twaddle et al., 2018b). If the administered gavage dose were retained within the luminal contents (as opposed to the enterocytes), the levels of As3 and As^i-bound would have been much higher in the unperfused intestine. Clearly, reductive and methylation metabolism within the intestine predominates. Repeated analysis of selected tissue samples stored at −60 °C over the course of several months showed no evidence for significant changes in the determined concentrations of DMA species, as detailed previously for blood components (Twaddle et al., 2018b).

2.4. Liquid chromatography

Ion exchange LC was performed using a Thermo UltiMate 3000 HPLC system (Thermo Scientific, Germering, Germany) consisting of a pump and autosampler. A Hamilton PRP-X100 column (4.1 × 250 mm, 10 μ particle size, Hamilton, Reno, NV), with an isocratic mobile phase consisting of 98% 10 mM ammonium phosphate (pH 8.25, prepared daily) and 2% methanol (Thermo Fisher Scientific) at a flow rate of 1 ml/min, was used for analyte separation/speciation.

2.5. Mass spectrometry

A Thermo X-Series II ICP-MS (Thermo Electron, Bremen, Germany), equipped with a microflow nebulizer and Peltier-cooled spray chamber maintained at 2 °C (PC3, Elemental Scientific, Omaha, NE), was operated in KED mode to monitor elemental arsenic (*m/z* 75) while

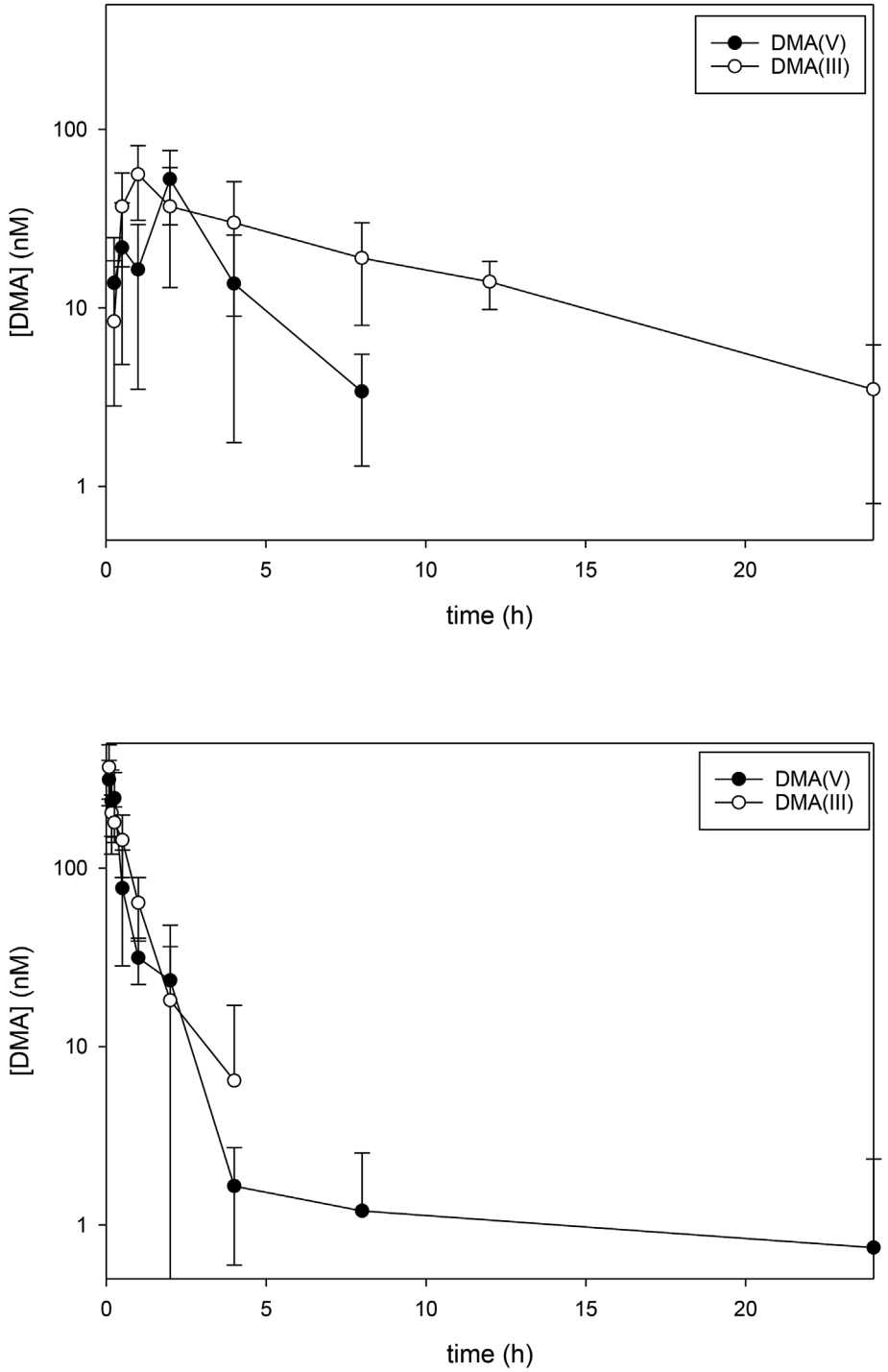

Fig. 2. Time course data for DMA species in erythrocytes from female CD-1 mice dosed orally or intravenously with 50 μg/kg bw DMA^V(arsenic equivalents). Note the common log abscissa scale and that the LODs were approximately 1 nM in blood (50 μL).
Top Panel: Oral administration; values plotted represent means of n =
6 mice per time point ± SD.
Bottom Panel. Intravenous administration; values plotted represent means of n =
5–
6 mice per time point ± SD.

mitigating potential mass interference (i.e., ArCl).

2.6. Sample calibration curve

Quantification of each sample set used a series of arsenic standards (arsenite, arsenate, MMA^V, DMA^V) in 10 mM ammonium phosphate (pH 8.25) at defined concentrations to prepare a daily calibration curve. Typically, these standards consisted of a blank along with 3–5 concentrations over a range of 0.05–20 ng/mL As. Linear responses were consistently observed ($R^2 > 0.999$). A typical sample set consisted of calibration standards, a buffer blank, matrix blanks, matrix spikes at multiple concentrations, and incurred samples. Standards were

Table 1
Toxicokinetic parameters in plasma from female CD-1 mice dosed orally with 50 μg/kg bw DMA^V (arsenic equivalents; values represent means of n = 6 mice per time point ± SD). Note that the fraction absorbed (absolute bioavailability) into plasma was determined from the ratio of DMA^V AUC-oral/DMA^V AUC-IV.

As Species	$t_{1/2Elim}$ (h)	$t_{1/2Abs}$ (h)	$AUC_{0-\infty}$ (nM x h)	C_{max} (nM)	T_{max} (h)	Fraction absorbed
DMA^V	4.7	0.8	400	84 ± 26	0.5	0.48

interspersed throughout the sample set to monitor ICP/MS and chromatographic performance. The column effluent was directed through a 10-port switching valve (Rheodyne/IDEX, Lake Forest, IL) that was used to introduce a post-column standard addition of arsenate to provide signal normalization throughout every sample set, as described previously (Twaddle et al., 2018a).

2.7. Method validation

Method validation consisted of spiking plasma or erythrocytes with 3 concentrations of mixed arsenic standards and preparing each concentration in quadruplicate (e.g., 0.1, 1.0, and 10.0 ng/mL) as described previously (Twaddle et al., 2018a). Similarly, tissues were spiked at 5, 10, and 100 ng/g with mixed arsenic standards and homogenized with 10 mg-equivalent aliquots analyzed in quadruplicate on separate days as described previously (Twaddle et al., 2018a).

Method detection limits for DMA species, which reflect the presence of low levels in untreated adult CD-1 mice (Table S1) that were subtracted from dosed samples, were approximately 1 nM in blood (50 μL) and 1 pmol/g in tissues (10 mg).

2.8. Toxicokinetic analysis

Plots of average blood (erythrocytes and plasma) concentrations of DMA species at each time (5–6 mice/time point) following bolus gavage and intravenous administration were analyzed using model-independent (non-compartmental) pharmacokinetic analysis (PK Solutions 2.0 software, Summit Research Services, Montrose, CO). Background levels were determined from buffer blanks and untreated (pre-dose) mouse blood (Table S1) and were subtracted from all time points prior to kinetic analysis in order to derive more accurately toxicokinetic parameters that are dependent on achieving complete elimination (e.g., $t_{1/2Elim}$, $AUC_{0-\infty}$, and clearance). All data points collected were used for the graphical analyses described. Log-linear plots were fit to up to three kinetic phases corresponding to elimination, distribution, and absorption/formation. The first-order elimination rate constants (k_{Elim}) were determined from the terminal slope of each curve. The first-order distribution and/or absorption rate constants were determined after subtracting the contribution from the terminal elimination phase of the respective curve (i.e., feathering). Half-times were determined from rate constants using the relationship: half-time ($t_{1/2}$) = ln 2/k. The areas under the time-concentration curve ($AUC_{0-\infty}$) for blood measurements were determined by using the trapezoidal rule.

2.9. Statistical analysis

Pharmacokinetic parameters were determined from plots of group mean values (n = 5–6 mice at each time point). Where appropriate, group mean values were compared by using a two-sided *t*-test. Significance was associated with p-value ≤ 0.05.

3. Results

3.1. Plasma toxicokinetics

3.1.1. Background exposure

Mice obtained from Charles River contained measurable levels of DMA species in blood and tissues. In order to reduce the contribution to blood and tissue levels from this background as much as practicable, upon arrival all mice were placed on a different chow-based diet with lower arsenic content (Purina 5K96) for at least 10 days. The levels of arsenic species present in this basal diet were reported previously (Twaddle et al., 2018a). The mean values ± SD were determined from 5 lots of feed for arsenite (16 ± 0.82 ppb), arsenate (26 ± 3.9 ppb), MMA^V (2 ± 0.2 ppb), DMA^V (17 ± 3.7 ppb), and arsenobetaine (45 ± 12 ppb). Consistent with the levels of arsenic species in the basal diet and previous publications (Twaddle et al., 2018a), blood and tissues from untreated mice (pre-dose) contained detectable levels of DMA^V and DMA^{III} (Twaddle et al., 2018b; Table S1). The respective background values were subtracted from blood and tissue levels determined after dosing in order to more accurately derive toxicokinetic parameters that are dependent on complete elimination (e.g., $t_{1/2Elim}$, $AUC_{0-\infty}$, and clearance).

3.1.2. Oral DMA^V dosing

Gavage treatment of mice with 50 μg/kg bw doses of DMA^V (i.e., 667 nmol As/kg bw) led to its rapid appearance in plasma, with maximal plasma concentration of DMA^V observed at 0.5 h (Fig. 1 and Table 1). No evidence for demethylation to MMA^V or As^i was observed (data not shown). Similarly, no evidence for formation of trimethylarsine oxide (TMAO) was observed in the LC-ICP/MS chromatograms (data not shown). The elimination of DMA^V from plasma was slower, with observable levels present at 24 h (Fig. 1 and Table 1). Analysis of samples with and without H_2O_2 showed that binding of DMA to plasma proteins contributed only a small amount to the total arsenic present (e.g., DMA^{III} levels were below 20% of DMA^V, not shown).

3.1.3. Intravenous DMA^V dosing

Intravenous injection of mice with 50 μg/kg bw of DMA^V led to rapid elimination that was approximately 6-fold faster than that observed from oral administration (Fig. 1 and Tables 1 and 2). Based on the $AUC_{0-\infty}$ values for oral and intravenous DMA^V, the absolute bioavailability was 48% (Tables 1 and 2). The observed volume of distribution for DMA^V (0.90 L/kg bw) is consistent with its distribution throughout total body water. There was also a large route effect on the elimination kinetics for DMA^V, with a much slower process observed following oral administration (Fig. 1).

3.2. Erythrocyte toxicokinetics

3.2.1. Oral DMA^V dosing

The pilot study established the utility of the erythrocyte fraction as an accessible source for measuring systemic trivalent arsenic species to complement the measurements of pentavalent arsenic species in mouse plasma (Twaddle et al., 2018a). Fig. 2 shows the time courses for bound DMA^{III} after oral administration and the corresponding concentrations of "free" DMA^V. As seen previously, the levels of DMA^V in the erythrocyte fraction were consistently lower than the corresponding levels

Table 2
Toxicokinetic parameters in plasma from female CD-1 mice dosed intravenously with 50 μg/kg bw DMA^V (arsenic equivalents; n = 5–6 per time point).

As Species	$t_{1/2Elim}$ (h)	$t_{1/2Distr}$ (h)	$AUC_{0-\infty}$ (nM x h)	Cl (L/(h x kg bw))	V_d (L/kg bw)
DMA^V	0.8	0.1	830	0.80	0.90

Table 3
Toxicokinetic parameters in erythrocytes from female CD-1 mice dosed orally with 50 μg/kg bw DMA^V (arsenic equivalents; n = 6 mice per time point, means ± SD). Note that fraction absorbed (absolute bioavailability) into erythrocytes was determined from the ratio of DMA^V AUC-oral/DMA^V AUV-IV.

As Species	$t_{1/2Elim}$ (h)	$AUC_{0-\infty}$ (nM x h)	C_{max} (nM)	T_{max} (h)	Fraction absorbed
DMA^V	1.0	138	53 ± 23	2	0.59
DMA^{III}	6.5	445	56 ± 25	1	–

Table 4
Toxicokinetic parameters for arsenic species in erythrocytes from female CD-1 mice dosed intravenously with 50 μg/kg bw DMA^V (arsenic equivalents; n = 5–6 per time point).

As Species	$t_{1/2Elim}$ (h)	$AUC_{0-\infty}$ (nM x h)
DMA^V	0.8	233
DMA^{III}	1.3	236

in plasma and the elimination kinetics were faster (Tables 1 and 3). The levels of DMA^{III} bound to erythrocyte thiols generally exceeded those of the corresponding "free" DMA^V, and the elimination was slower. Accordingly, the erythrocyte AUC for bound DMA^{III} was 3.2-fold higher than that for DMA^V (Table 3).

3.2.2. Intravenous DMA^V dosing

Injection of DMA^V led to binding of DMA^{III} bound to erythrocyte thiols at levels similar to those for "free" DMA^V and the elimination profiles were also similar (Tables 3 and 4; Fig. 2). Accordingly, the respective AUCs for DMA^V and DMA^{III} were similar (Tables 3 and 4). The erythrocyte-derived value for fraction of DMA^V absorbed (0.59) was similar to that from plasma data (Tables 1 and 3). When comparing IV and oral routes, the elimination kinetics for DMA^V were similar, but elimination of DMA^{III} was slower after oral administration. As a result, the respective AUC after oral administration for DMA^{III} was greater (1.9-fold), apparently at the expense of DMA^V.

3.2.3. Comparison between oral dosing with equimolar DMA^V vs. sodium arsenite from Twaddle et al. (2018b)

Oral administration with DMA^V produced lower plasma concentrations of DMA^V with the AUC and C_{max} values representing 45 and 38%, respectively, of those produced by oral dosing with equimolar arsenite (Twaddle et al., 2018b). The kinetics of DMA^V elimination in plasma were similar to those observed following oral administration of arsenite (Table 1, respectively; Twaddle et al., 2018b).

Erythrocyte toxicokinetics showed that orally administered DMA^V produced lower AUCs for both DMA^V (47%) and DMA^{III} (66%; Table 3 and Fig. 3) than the corresponding oral administration of arsenite (Twaddle et al., 2018b). Similarly, the AUCs for DMA^V and DMA^{III} from intravenously administered DMA^V were lower than the corresponding values from arsenite (57 and 24%, respectively). The elimination kinetics for DMA^V and DMA^{III} from erythrocytes were markedly faster for both routes of DMA^V administration when compared to arsenite administration.

3.3. Tissue measurements

3.3.1. Oral DMA^V dosing

DMA species were also measured in selected tissues following oral administration, including targets for carcinogenesis (liver, lung, and kidney), intestine, muscle, and brain (Fig. 4 and Table S3). A common time interval of 1 h after dosing was selected for comparison because this time produced maximal levels of DMA-derived species in liver, lung, and erythrocytes after oral dosing in the pilot study (Twaddle et al., 2018a) and were reported this way in the previous arsenite toxicokinetic study (Twaddle et al., 2018b). The percentages of administered dose as total DMA species within the tissues at the 1 h time point were estimated using literature values for several organs in adult female CD-1 mice (Krinke, 2004). Tissues contained very low percentages of the administered dose, in the range of 0.001% (brain) to 0.03% (liver). Blood content of total DMA species was estimated at 0.06% of the administered dose. Based on the previous study with arsenite dosing (Twaddle et al., 2018a), urine was collected over an 8 h period and contained 40–78% of administered dose (mean 53 ± 14%; primarily as DMA^V, 83%), whereas feces collected over a 24 h period contained 1–6% (mean 2 ± 2%%; primarily as DMA^V, 87%). Given the low percentages estimated in the blood and tissues, the preponderance of administered DMA^V dose is probably present in the urine, although urine was not collected for the current study. While the T_{max} values for DMA species were observed at other time points in the blood (Figs. 1 and 2), the use of a common time was simpler and, in any case, the ratio of tissue/plasma (partition or distribution ratio) can be computed for use in modeling.

Following oral administration, levels of bound DMA^{III} and DMA^V were highest in the intestine, relative to other tissues tested (Fig. 4). Liver, the organ receiving portal blood delivery following absorption in the intestine, had lower levels of DMA species than the intestine. Apparent first-pass reductive metabolism of DMA^V in the intestine and liver was suggested by the successively lower levels of bound DMA^{III} in intestine > liver > downstream sites like erythrocytes, lung, kidney, muscle, and brain. It is noteworthy that the levels of DMA species were much lower in brain than all other tissues examined. The time course of DMA levels after oral administration was investigated in the GI tract (Table S4), which showed that maximal levels DMA^V and DMA^{III} were observed at the initial sampling time (0.25 h), albeit with high variability, presumably associated with sampling conducted across the entire length of the intestine to avoid bias associated with sampling any one region.

3.3.2. Intravenous DMA^V dosing

Tissue measurements were made in intestine, liver, and erythrocytes following IV injection to evaluate the effects of first-pass metabolism (Fig. 4 and Table S5). Following IV administration, the levels of bound DMA^{III} and DMA^V were lower in the intestine and liver than those produced by oral administration (Fig. 4), whereas the plasma and erythrocyte levels were similar for both routes. All tissue levels after intravenous injection were similar (Fig. 4 and Table S5). This result contrasts what was seen after oral administration where the levels of bound DMA^{III} successively decreased in the order of entry into the body (i.e., intestine > liver > erythrocytes; Fig. 4 and Table S3).

3.3.3. Comparison of tissue levels between oral dosing with equimolar DMA^V vs. sodium arsenite from Twaddle et al. (2018b)

The levels of bound DMA^{III} in the intestine were similar for gavage administration of DMA^V vs. sodium arsenite (89%); however, in liver (10%) and all other tissues examined (12–41%) the respective levels were lower in mice dosed with DMA^V (Table S2). The relative tissue levels of DMA^V showed a similar pattern (76% of the arsenite value in the intestine and 17–41% range in the other tissues).

4. Discussion

Previous studies of bolus oral dosing with sodium arsenite in adult female CD-1 mice provided a framework for sample collection and analysis to generate toxicokinetic data for pentavalent and bound trivalent arsenic species in blood and tissues (Twaddle et al., 2018a, 2018b). The predominant species observed in plasma and urine was the terminal product of As3MT methylation and aerobic oxidation, DMA^V (Scheme). Similarly, DMA^{III} was the predominant species present bound to tissue and erythrocyte thiols after oral dosing with arsenite (Twaddle

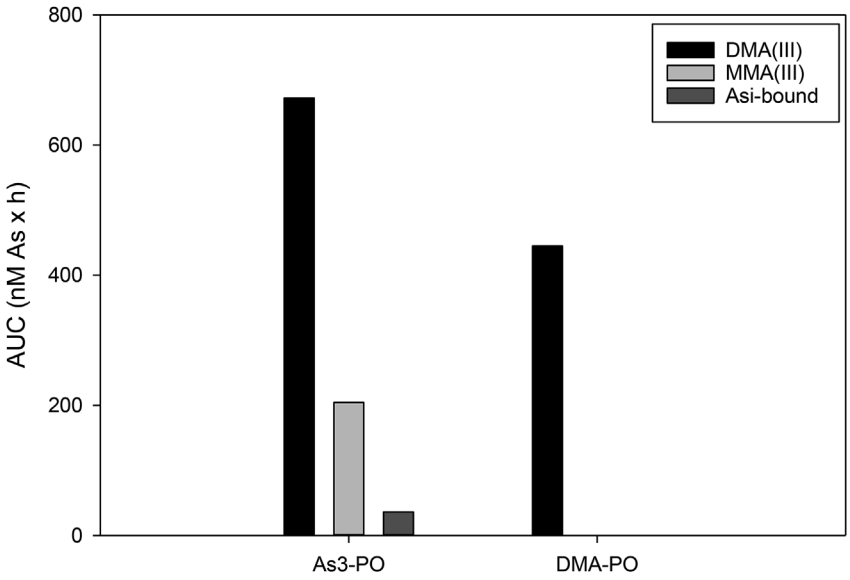

Fig. 3. Comparison of erythrocyte AUCs (areas under time-concentration curves) for bound trivalent arsenic species produced after oral administration (PO) with equimolar doses of either arsenite (As3-PO; Twaddle et al., 2108b) or DMA^V (DMA-PO; Table 3). Note that the AUC parameters are derived from measurements in multiple mice at each time point in the time-concentration profile and, therefore, represent composite values and cannot reflect inter-animal variability.

et al., 2018b). The kinetic and thermodynamic factors associated with arsenic-sulfur bonding were manifested in the time courses for blood and tissue levels as: 1) high fluxes of trivalent and pentavalent arsenic metabolites in the intestine and liver through the action of As3MT; 2) extensive binding of trivalent arsenic species to tissue and erythrocyte thiols; 3) facile mobilization of bound trivalent arsenic species by physiological levels of GSH; and 4) reduction of pentavalent arsenic species to the trivalent analogs by cellular constituents in tissues (Delnomdedieu et al., 1994; Stýblo et al., 1997; Németi and Gregus, 2013; Twaddle et al., 2018a, 2018b). The formation and fate of DMA species appear pivotal in understanding the toxic effects of arsenic in humans and animal models because they occupy a central role in the metabolism and disposition of As^i. In addition, DMA^V and As^i share a similar magnitude of human dietary exposures (Oguri et al., 2014; U.S. Food and Drug Administration, 2016) and carcinogenicity in adult rodent models (Wei et al., 2002; Arnold et al., 2006; Tokar et al., 2012; Cohen et al., 2013). For these reasons, it was important to compare the extent to which As3MT-dependent methylation of inorganic arsenic and reductive metabolism of DMA^V contribute to production of the reactive metabolite, DMA^{III}, which can bind covalently to tissue thiols and potentially dysregulate cellular functions (Go and Jones, 2013; Shen et al., 2013). This study enabled such a comparison by conducting toxicokinetic studies in the same animal model treated with either sodium arsenite or DMA^V under identical conditions of dosing and analysis.

4.1. Toxicokinetics of DMA^V in adult female CD-1 mice following gavage and injection routes of administration

Comparison of DMA^V blood toxicokinetics by oral and intravenous routes showed clear evidence for pre-systemic metabolism of DMA^V in the intestine and liver (Fig. 4), which led to an absolute (oral) bioavailability of 48% (Tables 1 and 2). These findings seemingly contrast with those of Vahter et al. (1984) where radiolabeled DMA^V (oral administration of 0.4 mg/kg bw) was recovered quantitatively in mouse excreta within 48 h, predominately as unchanged parent in urine (84%) and feces (16%). However, plasma measurements of DMA^V do not include the portion of dose converted to DMA^{III}, which binds to thiols in erythrocytes and tissues (Twaddle et al., 2018b). Bound levels of the reactive metabolite, DMA^{III}, in the orally exposed intestine were far greater than in any other tissue examined (especially the IV-exposed intestine), which suggests significant reduction after bolus delivery at the initial site of entry, from which mobile thiol complexes could distribute into the liver and further, systemically. Consistent with this view, liver and erythrocytes, which contain significant pools of available thiol residues from small molecules and proteins (Twaddle et al., 2018a), contained significant amounts of bound DMA^{III}. Major organs like the lung and kidney contained levels similar to those in liver, while brain and muscle had the lowest levels (Fig. 5). After IV administration, the erythrocyte AUCs for DMA^V and bound DMA^{III} were similar (Table 4), but after gavage the AUC for bound DMA^{III} was ~3-fold higher than DMA^V (Table 3). These results show that systemic reductive metabolism of DMA^V does occur after injection, but to a lesser extent than after successive passage through the intestine and liver after gavage. The rapidity of systemic appearance for DMA^{III}, as evidenced by the time course for binding in erythrocytes (Fig. 2 and Table 3), suggests that the reduction, soluble complex formation, and transport into blood takes place after absorption into the intestine as opposed to reduction by anaerobic colonic microbiota after transit through the gastrointestinal tract.

4.2. Comparison of toxicokinetics of DMA^V and sodium arsenite in adult female CD-1 mice following oral administration

Gavage treatment of adult female CD-1 mice with sodium arsenite led to extensive methylation, predominately to the terminal metabolite, DMA^V, with smaller amounts of the intermediate, MMA^V, and minor amounts of the substrate, arsenite, in plasma (Twaddle et al., 2018b). "Free" DMA^V represented > 98% of combined plasma AUCs for arsenic species. Measurements in tissues and erythrocytes provided evidence for the formation and binding of reactive metabolites, DMA^{III} and MMA^{III}, as well as arsenite. Bound DMA^{III} comprised 74% of the combined AUCs in erythrocytes while bound MMA^{III} comprised 22%. DMA^{III} was the major bound metabolite in all tissues except the intestine, where MMA^{III} was maximal. Since DMA^{III} is the final product of arsenite methylation by As3MT (Dheeman et al., 2014; Scheme) at low doses (this work and Hughes et al., 2008), and it rapidly reacts with thiol groups, it is possible that soluble trivalent complexes could circulate systemically and exchange with other thiols at distal sites. In addition, in situ reduction of DMA^V within tissues is also likely (Delnomdedieu et al., 1994; Stýblo et al., 1997; Németi and Gregus, 2013; Twaddle et al., 2018a, 2018b), which also contributes to tissue binding (this study).

For this reason, the current study focused on dosing with DMA^V so that only the reductive pathway was possible (Scheme). The plasma AUC for DMA^V after DMA^V dosing was 45% of that from arsenite (Table 1) and the erythrocyte AUC for bound DMA^{III} was 66% of that

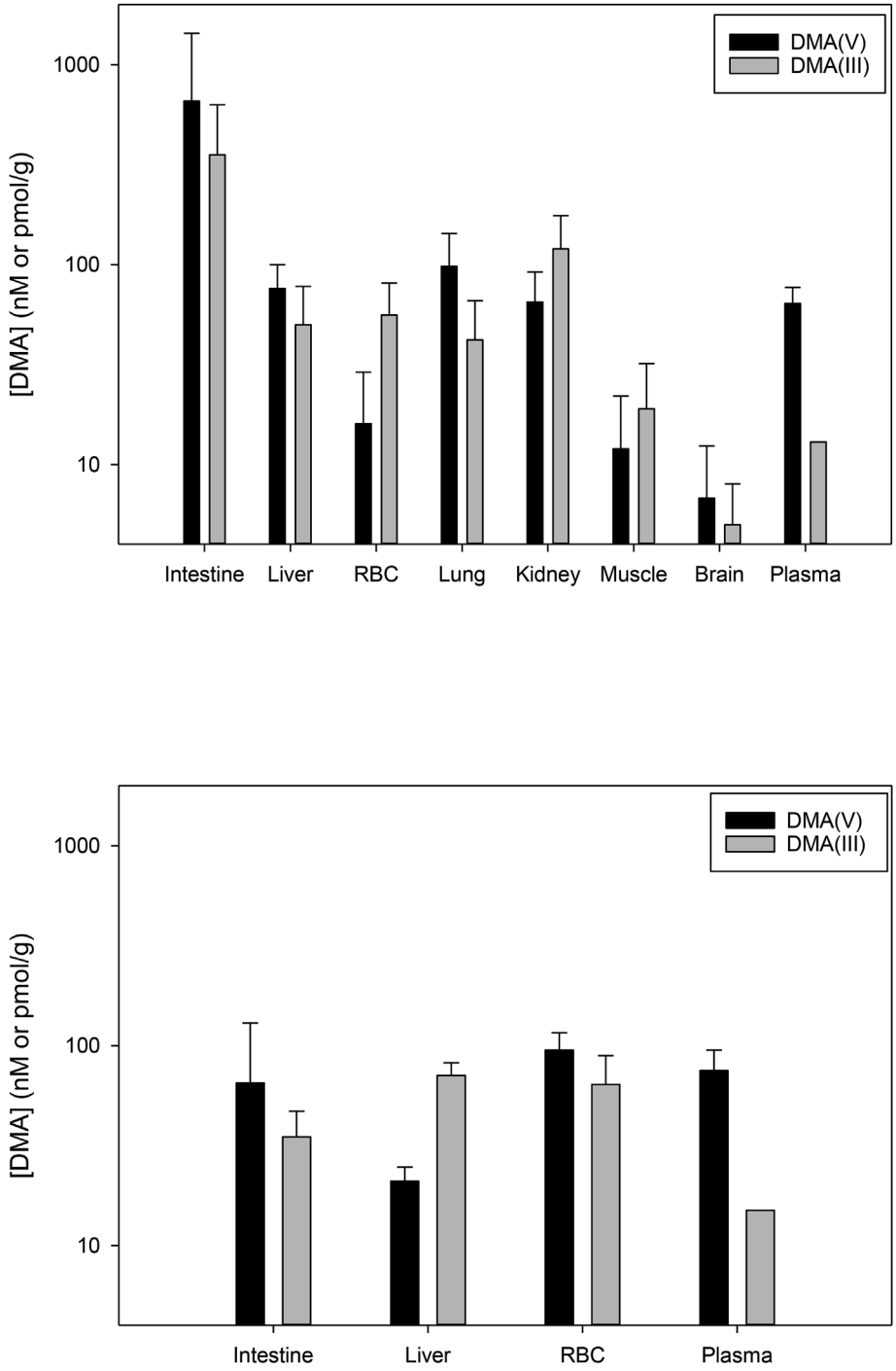

Fig. 4. Tissue concentrations for DMA species from female CD-1 mice 1 h after oral or intravenous dosing with 50 μg/kg bw DMA^V (arsenic equivalents). Note the common log abscissa scales, the LODs were approximately 1 nM in blood (50 μL) and 1 pmol/g in tissues (10 mg), and that the plasma concentration of DMA^{III} was estimated as < 20% of the plasma DMA^V.
Top Panel: Oral administration; mean values ± SD; n = 6 mice.
Bottom Panel: Intravenous administration; mean values ± SD; n = 5–6 mice.

from arsenite (Fig. 3). However, in the intestine where reductive metabolism first occurs, both DMA^V (76%) and bound DMA^{III} (89%) were more similar for DMA^V vs. arsenite dosing (Tables S2 and S3). While the respective percentage of bound DMA^{III} in liver was 10% for DMA^V vs. arsenite gavage, in lung it was 71%, and in kidney 20%. Fig. 3 also shows the smaller contributions to erythrocyte AUCs for bound MMA^{III} and arsenite after arsenite dosing.

There are notable differences in the structures of arsenic species that affect interactions integral to tissue uptake and efflux of As^i and methylated species. Firstly, arsenite is neutral at physiological pH values (pKa 9.2), whereas DMA^V (pKa 6.2) and arsenate (pKa 2.2) are negatively charged. While arsenite, arsenate, and DMA^V are all small polar molecules, the charge structures affect interactions with transporter proteins (reviewed in Roggenbeck et al., 2016). For example, arsenite is a preferential substrate for aquaporins (AQP), which transport neutral substrates like water and glycerol, and arsenate interacts with phosphate transporters. On the other hand, DMA^V is a substrate for multidrug resistance proteins (MRP), which often transport negatively

charged glucuronide/sulfate/glutathione conjugates. The transcellular and paracellular interactions of arsenic species in the intestine are especially important for understanding absorption processes integral to oral bioavailability, but at this time limited information is available to fully compare relevant biochemical pathways for inorganic and methylated arsenic species (Roggenbeck et al., 2016; Calatayud et al., 2012).

Furthermore, differences in reaction kinetics and the potential for structural effects on modified proteins from mono-thiol binding of DMA^{III} vs. *bis*- and *tris*-interactions of MMA^{III} and arsenite, respectively, could also influence relative toxic potential (Shen et al., 2013). Irrespective of the source for DMA^{III} exposure (i.e., indirectly from arsenite metabolism or directly from ingestion of DMA^{V}), the levels of bound DMA^{III} found in circulation and most tissues only differ by degree (Figs. 3–4 and Tables S2–S3), particularly in target tissues for carcinogenesis (i.e., liver, lung, and kidney).

5. Conclusions

The current study expands upon our previous toxicokinetic studies in an important animal model for the carcinogenic effects of arsenite (Tokar et al., 2011) and DMA^{V} (Tokar et al., 2012). The data are consistent with a scenario in which ingested DMA^{V} is extensively absorbed into the gut, where a significant portion undergoes rapid first-pass reductive metabolism to reactive DMA^{III}, which binds to protein and low molecular weight thiols. The remaining DMA^{V} and mobile DMA^{III}-thiol complexes are then transported via portal blood flow to the liver for additional reduction and systemic distribution. Dosing with DMA^{V} produced fluxes of reactive DMA^{III} in tissues and blood from reductive metabolism that were nearly as high as those produced by methylation-dependent metabolism of sodium arsenite. The especially high levels of bound DMA^{III} in intestinal tissue from ingestion of either As^{i} or DMA^{V} support reports of adverse effects, including transformation of intestinal cells (Chiocchetti et al., 2019) and changes in gut microbiota and immune functions (Gokulan et al., 2018). The levels of bound trivalent arsenic metabolites in target tissues (i.e., liver, lung, and kidney) are supportive of the carcinogenic effects of both As^{i} and DMA^{V} in chronically exposed rodent models (Wei et al., 2002; Arnold et al., 2006; Tokar et al., 2011, 2012; Cohen et al., 2013). These results provide direct evidence for metabolic activation of DMA^{V} by reduction and, by inference, As^{i} through both methylation and reduction pathways. These blood/tissue concentration data on the kinetics and metabolism of DMA^{V} should be useful in physiologically based pharmacokinetic (PBPK) modeling of DMA^{V}, arsenite metabolism, and the disposition of DMA^{III} as the major reactive metabolite (Evans et al., 2008). Finally, these results validate the notion that risk assessments, currently associated with As^{i} intake in drinking water and food, should be expanded to include dietary DMA^{V}.

Conflicts of interest

The authors declare that there are no conflicts of interest.

Declaration of interests

The authors declare that they have no known competing financial interests or personal relationships that could have appeared to influence the work reported in this paper.

Acknowledgements

This study was funded by the National Toxicology Program under an Interagency Agreement between FDA and NIEHS (FDA IAG # 224-17-0502). The authors gratefully acknowledge Dr. Anil Patri, NCTR, for generous access to ICP/MS instrumentation in the NCTR/ORA Nanotechnology Laboratory. The views presented in this article do not necessarily reflect those of the U.S. Food and Drug Administration.

Appendix A. Supplementary data

Supplementary data to this article can be found online at https://doi.org/10.1016/j.fct.2019.04.045.

References

Al Amin, M.H., Xiong, C., Glabonjat, R.A., Francesconi, K.A., Oguri, T., Yoshinaga, J., 2018. Estimation of daily intake of arsenolipids in Japan based on a market basket. Food Chem. Toxicol. 118, 245–251.
Arnold, L.L., Eldan, M., Nyska, A., van Gemert, M., Cohen, S.M., 2006. Dimethylarsinic acid: results of chronic toxicity/oncogenicity studies in F344 rats and B6C3F1 mice. Toxicology 223, 82–100.
Calatayud, M., Vázquez, M., Devesa, V., Vélez, D., 2012. In vitro study of intestinal transport of inorganic and methylated arsenic species by Caco-2/HT29-MTX co-cultures. Chem. Res. Toxicol. 25, 2654–2662.
Chiocchetti, G.M., Vélez, D., Devesa, V., 2019. Effect of chronic exposure to inorganic arsenic on intestinal cells. Toxicol. Lett. 286, 80–88.
Cohen, S.M., Arnold, L.L., Beck, B.D., Lewis, A.S., Eldan, M., 2013. Evaluation of the carcinogenicity of inorganic arsenic. Crit. Rev. Toxicol. 43, 711–752.
Currier, J.M., Douillet, C., Drobná, Z., Stýblo, M., 2016. Oxidation state specific analysis of arsenic species in tissues of wild-type and arsenic (+3 oxidation state) methyltransferase-knockout mice. J. Environ. Sci. 49, 104–112.
Delnomdedieu, M., Basti, M.M., Stýblo, M., Otvos, J.D., Thomas, D.J., 1994. Complexation of arsenic species in rabbit erythrocytes. Chem. Res. Toxicol. 7, 621–627.
Dheeman, D.S., Packianathan, C., Pillai, J.K., Rosen, B.P., 2014. Pathway of human AS3MT arsenic methylation. Chem. Res. Toxicol. 27, 1979–1989.
European Food Safety Authority, 2009. Scientific opinion on arsenic in food. EFSA J 7, 1351. http://www.efsa.europa.eu/en/efsajournal/pub/1351.
Evans, M.V., Dowd, S.M., Kenyon, E.M., Hughes, M.F., and El-Masri, H. A physiologically based pharmacokinetic model for intravenous and ingested dimethylarsinic acid in mice. Toxicol. Sci. 104, 250-260.
Glabonjat, R.A., Raber, G., Jensen, K.B., Ehgartner, J., Francesconi, K.A., 2014. Quantification of arsenolipids in the certified reference material NMIJ 7405-a (Hijiki) using HPLC/mass spectrometry after chemical derivatization. Anal. Chem. 86, 10282–10287.
Go, Y.-M., Jones, D.P., 2013. Thiol/disulfide redox states in signaling and sensing. Crit. Rev. Biochem. Mol. Biol. 48, 173–191.
Gokulan, K., Arnold, M.G., Jensen, J., Vanlandingham, M., Twaddle, N.C., Doerge, D.R., Cerniglia, C.E., Khare, S., 2018. Exposure to arsenite in CD-1 mice during juvenile and adult stages: effects on intestinal microbiota and gut-associated immune status. mBio 9, 18 e01418.
Hughes, M.F., Devesa, V., Adair, B.M., Conklin, S.D., Creed, J.T., Stýblo, M., Kenyon, E.M., Thomas, D.J., 2008. Tissue dosimetry, metabolism and excretion of pentavalent and trivalent demethylated arsenic in mice after oral administration. Toxicol. Appl. Pharmacol. 227, 26–35.
Kenyon, E.M., Del Razo, L.M., Hughes, M.F., 2005. Tissue distribution and urinary excretion of inorganic arsenic and its methylated metabolites in mice following acute oral administration of arsenate. Toxicol. Sci. 85, 468–475.
Kobayashi, Y., Hayakawa, T., Hirano, S., 2007. Expression and activity of arsenic methyltransferase Cyt19 in rat tissues. Environ. Toxicol. Pharmacol. 23, 115–120.
Krinke, G.J., 2004. Ch. 9 normative histology of organs. In: Hedrich, H., Bullock, S., Pertusz, P. (Eds.), The Handbook of Experimental Animals: the Laboratory Mouse, pp. 135.
Mukherjee, A., Sengupta, M.K., Hossein, M.A., Ahamed, S., Das, B., Nayak, B., Lodh, D., Rahman, M.M., Chakraborti, D., 2006. Arsenic contamination in groundwater: a global perspective with emphasis on the Asian scenario. J. Health Popul. Nutr. 24, 142–163.
Németi, B., Gregus, Z., 2013. Reduction of dimethylarsinic acid to the highly toxic dimethylarsinous acid by rats and rat liver cytosol. Chem. Res. Toxicol. 26, 432–443.
Oguri, T., Yoshinaga, J., Tao, H., Nakazato, T., 2014. Inorganic arsenic in the Japanese diet: daily intake and source. Arch. Environ. Contam. Toxicol. 66, 100–112.
Raml, R., Raber, G., Rumpler, A., Bauernhofer, T., Goessler, W., Francesconi, K.A., 2009. Individual variability in the human metabolism of an arsenic-containing carbohydrate, 2', 3'-dihydroxypropyl 5-deoxy-5-dimethylarsinoyl-β-D-riboside, a naturally occurring arsenical in seafood. Chem. Res. Toxicol. 22, 1534–1540.
Roggenbeck, B.A., Banerjee, M., Leslie, E.M., 2016. Cellular arsenic transport pathways in mammals. J. Environ. Sci. 49, 38–58.
Schmeisser, E., Goessler, W., Francesconi, K.A., 2006. Human metabolism of arsenolipids present in cod liver. Anal. Bioanal. Chem. 385, 367–376.
Shen, S., Li, X.-F., Cullen, W.R., Weinfeld, M., Le, X.C., 2013. Arsenic binding to proteins. Chem. Rev. 7769–7792.
Spuches, A.M., Kruszyna, H.G., Rich, A.M., Wilcox, D.E., 2005. Thermodynamics of the As (III)-thiol interaction: arsenite and monomethylarsenite complexes with glutathione, dihydrolipoic acid, and other thiol ligands. Inorg. Chem. 44, 2964–2972.
Stýblo, M., Serves, S.V., Cullen, W.R., Thomas, D.J., 1997. Comparative inhibition of yeast glutathione reductase by arsenicals and arsenothiols. Chem. Res. Toxicol. 10, 27–33.
Taylor, V., Goodale, B., Raab, A., Schwerdtle, T., Reimer, K., Conklin, S., Karagas, M.R., Francesconi, K.A., 2017. Human exposure to organic arsenic species from seafood.

Sci. Total Environ. 580, 266–282.
Tokar, E.J., Diwan, B.A., Ward, J.M., Delker, D.A., Waalkes, M.P., 2011. Carcinogenic effects of “whole-life” exposure to inorganic arsenic in CD1 mice. Toxicol. Sci. 119, 73–83.
Tokar, E.J., Biwan, B.A., Waalkes, M.A., 2012. Renal, hepatic, pulmonary and adrenal tumors induced by prenatal inorganic arsenic followed by dimethylarsinic acid in adulthood in CD1 mice. Toxicol. Lett. 209, 179–185.
Twaddle, N.C., Vanlandingham, M., Churchwell, M.I., Doerge, D.R., 2018a. Metabolism and disposition of arsenic species from controlled dosing with sodium arsenite in adult female CD-1 mice. I. Pilot study to determine dosing, analytical measurements, and sampling strategies. Food Chem. Toxicol. 111, 482–493.
Twaddle, N.C., Vanlandingham, M., Fisher, J.W., Doerge, D.R., 2018b. Metabolism and disposition of arsenic species from controlled dosing with sodium arsenite in adult female CD-1 mice. III. Toxicokinetic studies following oral and intravenous administration. Food Chem. Toxicol. 121, 676–686.
Twaddle, N.C., Vanlandingham, M., Beland, F.A., Fisher, J.W., Doerge, D.R., 2019. Metabolism and disposition of arsenic species from oral dosing with sodium arsenite in neonatal CD-1 mice. IV. Toxicokinetics following gavage administration and lactational transfer. Food Chem. Toxicol. 123, 28–41.
U.S. Environmental Protection Agency, 2010. Toxicological Review of Inorganic Arsenic. https://cfpub.epa.gov/ncea/iris_drafts/recordisplay.cfm?deid=219111.
U.S. Food and Drug Administration Center for Food Safety and Applied Nutrition, 2016. Arsenic in Rice and Rice Products Risk Assessment Report. https://www.fda.gov/downloads/Food/FoodScienceResearch/RiskSafetyAssessment/UCM486543.pdf.
Vahter, M., Marafante, E., Dencker, L., 1984. Tissue distribution and retention of ^{74}As-dimethylarsinic acid in mice and rats. Arch. Environ. Contam. Toxicol. 13, 259–264.
Wei, M., Wanibuchi, H., Morimura, K., Iwai, S., Yoshida, K., Endo, G., Kakae, D., Fukushima, S., 2002. Carcinogenicity of dimethylarsinic acid in male F344 rats and genetic alterations in induced urinary bladder tumors. Carcinogenesis 23, 1387–1397.
Wolle, M.M. and Conklin, S.D. 2108. Speciation analysis of arsenic in seafood and seaweed: Part II - single laboratory validation of method. Anal. Bioanal. Chem. 410, 5689-5702.
World Health Organization, 2011. Safety evaluation of certain contaminants in food. Arsenic. WHO Food Additive Series, vol. 63. pp. 153–316.
Zhao, F.-J., Zhu, Y.-G., Meharg, A.A., 2013. Methylated arsenic species in rice: geographical variation, origin, and uptake mechanisms. Environ. Sci. Technol. 47, 3957–3966.
Zhu, Y.-G., Yoshinaga, M., Zhao, F.-J., Rosen, B.P., 2014. Earth abides arsenic biotransformations. Annu. Rev. Earth Planet Sci. 42, 443–467.